Microfluidics and Nanofluidics (2023) 27:38
https://doi.org/10.1007/s10404-023-02647-2

RESEARCH

Influence on the magnetic field on the scale formation in a microfluidic channel under a low Reynolds number flow

Chiung-Yi Huang[1] · **Che-Hsin Lin**[1]

Received: 3 February 2023 / Accepted: 26 April 2023 / Published online: 11 May 2023

Abstract

This study presents an external magnetic array to rapidly investigate the calcium carbonate formation in a microfluidic channel. The system comprises a copper coil capillary serving as the heat exchanger, a high-precision thermostatic water tank, a magnetic drive pump, and an external magnetic array. Various factors were considered during the experiment, including different concentrations (3 mM and 10 mM) of the test solution, magnetic treatment efficiency (magnet length 4.0 cm and 14.0 cm, treatment time 24 h and 72 h), and temperatures ranging from 25 ℃ to 50 ℃. The concentration of calcium ions, electrical conductivity, and pH value were measured to monitor subtle changes during water treatment. Additionally, particle size distribution and morphology of calcium carbonate were analyzed using SEM and XRD under various magnetic treatments. The experimental results revealed that (1) applying a magnetic field to the solution in a microfluidic channel under low Reynolds number flow led to a decrease in the particle size of calcium carbonate, (2) aragonite did not form in the microfluidic channel, and (3) the physicochemical properties of the solution remained unaltered by the magnetic treatment. Consequently, the reduction in particle size can prevent blockage in microchannels, providing an alternative solution to mitigate scaling issues in micro-heat exchangers.

Keywords Magnetic treatment · Anti-scale · Microfluidics · Particle size distribution · Laminar flow

Abbreviations

$CaCl_2$	Calcium chloride
$CaCO_3$	Calcium carbonate
DI water	Deionized water
ID	Inner diameter
EC	Electric conductivity
MEMS	Micro-electro-mechanical systems
MF	Magnetic field
$NaHCO_3$	Sodium bicarbonate
OD	Outer diameter
PE	Polyethylene
PSD	Particle size distribution
Re	Reynolds number
SEM	Scanning electron microscope
XRD	X-ray diffraction
W/O	Without

✉ Che-Hsin Lin
chehsin@mail.nsysu.edu.tw

[1] Department of Mechanical and Electro-Mechanical Engineering, National Sun Yat-sen University, No. 70, Lianhai Rd., Gushan Dist., Kaohsiung City 804201, Taiwan ROC

1 Introduction

Scale formation can have devastating effects on both industrial and household settings. The formation of scale typically results from the use of hard water, which contains various ions and is utilized as a heat carrier in heat exchangers. Calcium and magnesium ions are the primary culprits responsible for causing scale formation (Alabi et al. 2015), with calcium carbonate being the most commonly encountered constituent in piping systems (Zhang et al. 2001). This is because the solubility of calcium carbonate is strongly dependent on temperature (Coto et al. 2012). During the initial stages of scale formation, the structure is relatively loose, but over time, the scale becomes thicker and denser (Cho et al. 1997). Once the thickness of the scale reaches 25 mm, the heat conduction efficiency is reduced to 95% (Baker and Judd 1996). In severe cases, scale buildup can cause machine failure due to overheating, which can have serious consequences.

With the advancement of micro-electro-mechanical systems (MEMS), various micromachining methods have been developed for building microdevices (Lee et al. 2009; Osman et al. 2012; Zhu et al. 2019). Micro heat exchangers

play a crucial role in cooling and temperature control of these microdevices, offering the advantage of high heat transfer area per unit volume compared to conventional heat exchangers (Jiang et al. 2001; Mehendale et al. 2000). In general, the micro heat exchangers with micro machined channels of 220 µm in diameter did not experience particle deposition on the microchannel walls. This is attributed to the higher fluid shear near the microchannel walls (Perry and Kandlikar 2008). Alternatively, the scales form in the dead-volume region such that the scale deposition becomes more problematic for microfluidic systems (Marshall and Renjitham 2015; Mayer et al. 2012). Traditional methods for scale prevention include mechanical, chemical, and physical techniques (Müller-Steinhagen et al. 2011). Mechanical methods like milling, drilling, and scrubbing are effective for scale removal in larger heat exchangers but are challenging to apply in microsystems due to limited access to microchannels. Chemical methods rely on ion exchange, pH control, and chemical scale inhibitors, which are effective but can have negative environmental impacts such as eutrophication and aquatic life suffocation (Hasson et al. 2011; MacAdam and Parsons 2004), and may produce unintended byproducts due to chemical reactions. Physical techniques for anti-scaling mainly involve ultrasonic (Benzinger et al. 2005) and magnetic methods (Martínez Moya and Boluda Botella 2021), which do not directly contact the aqueous solution but alter the behavior of scale formation (Kozic and Lipus 2003). Ultrasonic methods can prevent scale attachment to the pipe walls but may induce localized regions of extreme temperature and pressure through inertial cavitation, leading to increased temperature and decreased solubility of calcium carbonate, resulting in scale formation in microsystems (Hotrum et al. 2015).

The consensus in the literature on magnetic water treatment for anti-scale is that it leads to more calcium carbonate crystals precipitating in the bulk fluid instead of depositing on the heat exchanger surface (Cho et al. 2003). Additionally, the presence of a magnetic field has been found to result in a higher portion of aragonite in the scale, which forms a sludge-like layer that is easy to wash away (Kozic and Lipus 2003). Aragonite and calcite are both crystalline phases of anhydrous calcium carbonate that are commonly found during scale formation. Calcite is the most thermodynamically stable form, while aragonite has a higher ground electronic state. Therefore, to form aragonite, the ions of calcium and carbonate need to have higher kinetic energies to overcome the repulsive forces of the potential barrier. This is why aragonite tends to form at higher temperatures or in the presence of magnetic fields (Kobe et al. 2002; Martínez Moya and Boluda Botella 2021). Previous literature on magnetic water treatment has also shown that it can re-orientate ions (Al Helal et al. 2018), result in smaller particle sizes (Silva et al. 2015; Xuefei et al. 2013; Zhao et al. 2014), alter morphology (Coey and Cass 2000), and further prevent scaling in a heat exchanger (Cho et al. 1998; Xuefei et al. 2013). Magnetic anti-scale devices are generally made up of either electromagnets or permanent magnets (Alabi et al. 2015). Permanent magnets have advantages over electromagnets in that they provide a static magnetic field to the solution and do not require additional power after installation in the system (Jiang et al. 2015). Moreover, higher applied magnetic field strength resulted in slower scale growth (Tai et al. 2008). Various materials can be used to make magnets, such as neodymium, samarium cobalt (SmCo), alnico, and ceramics, and the choice of material is a key factor in determining the magnetic flux intensity of a magnet. Among these materials, neodymium-type magnets have a higher flux density compared to other types of magnets with the same magnetic field strength (Al Helal et al. 2018). Different magnet arrangements have been proposed for anti-scale devices in previous studies. It has been reported that the alternate magnet arrangement is more effective in preventing scale compared to the non-alternate arrangement, and increasing the number of magnet pairs decreases the scaling power (Gabrielli et al. 2001). Therefore, it is feasible to increase the exposure time of the solution to the magnetic field by decreasing the system flow rate, which results in a laminar flow. Setting up the magnetic anti-scale devices in laminar flow is also suggested to be more effective in achieving the desired effect (Ignatov and Mosin 2014). Moreover, applying a smaller flow rate (laminar flow) is beneficial for saving energy, which is an important aspect of the magnetic method in addition to its environmental friendliness. Furthermore, laminar flow can be easily achieved in a microfluidic system, and the magnetic gradient in the microchannel is much more stable compared to the macrosystem, as the strength of the magnetic field is inversely proportional to the square of the distance (Chibowski and Szcześ 2018). Therefore, magnetic water treatment is considered as an alternative anti-scale solution for microsystem applications. However, there is a lack of literature discussing the influence of magnetic fields on calcium carbonate formation in a microfluidic channel under low Reynolds number flow. Further research in this area is needed.

In this study, a microfluidic heat exchange system was constructed with an external magnetic array to examine the impact of different conditions, such as magnet length and treatment time, on the particle size distribution and morphology of calcium carbonate, and their effect on magnetic treatment efficiency for scale formation. Throughout the experiment, parameters such as calcium ion concentration, electrical conductivity, and pH value were meticulously recorded. The system was comprised of a copper coil capillary as a heat exchanger, a high-precision thermostatic water tank, a magnetic drive pump, and an external magnetic array, which facilitated long-term experiments. Due

to the small diameter of the microsystem (2.0 mm, 4.0 mm) and the conducted flow rate (50 cc/min), a low Reynolds number was achieved ($Re = 264, 528$). Scanning electron microscopy (SEM) and X-ray diffraction (XRD) techniques were employed to analyze the particle size distribution and morphology of calcium carbonate.

2 Materials and methods

2.1 System overview

This study is to investigate the scale formation under the influence of the magnetic field in a microfluidic channel under a low Reynolds number. The experimental system is schematically illustrated in Fig. 1a. In general, the scale formation is only problematic when temperature increases abruptly. The solubility of calcium carbonate at 35 °C is around 5×10^{-2} Mol·kg^{-1}, and it decreases to its 75% and 56% for the temperature of 50 °C and 60 °C, respectively (Jun et al. 2018). Nevertheless, the temperature of the circulation water in a typical heat exchanger system is around 30~50 °C. For the temperature higher than 60 °C, the scale formation is too fast to be controlled due to the rapid water evaporation. Therefore, this study chose 50 °C and threated with different time periods and magnetic durations. The artificial hard water solutions were the synthesis of sodium bicarbonate and calcium chloride (Showa Chemical Co., LTD) prepared in DI water, and two different concentrations were conducted in this study, which were 10 mM and 3 mM ($NaHCO_3$:$CaCl_2$ = 1:1). As both concentrations resulted in supersaturated solutions, the solutions were filtered through a 1 µm pore size membrane immediately after mixing. The filtered solution, totaling 2 L, was stored in a reservoir and then circulated into the heat exchange system using a magnet pump (MD-6K-N18, Iwaki, Japan). The external magnetic array was employed to treat the solution prior to entering the copper coil capillary, allowing for magnetic treatment of the ions and molecules in the water before heating. The copper coil capillary used had an inner diameter (ID) of 2.0 mm and an outer diameter (OD) of 3.2 mm, with a length of 1.0 m, and was immersed in a thermostatic water bath (WB212-B1, TKS, Taiwan) set at 50 ℃.

The heated water bath provided heat to the test solution through the copper coil, which is known for its excellent thermal conductivity. As the test solution was heated, the solubility of calcium carbonate gradually decreased, leading to precipitation. The heated test solution, containing calcium carbonate crystals, was then returned to the reservoir after passing through the copper capillary. This process was repeated as the test solution in the reservoir re-entered the system. The scaling samples of calcium carbonate were collected from hydrophilic glass slides (1.0×1.0 cm^2) placed in the reservoir after the system ran for either 24 h or 72 h. It was observed that calcite and aragonite remained suspended in the solution for 30 days without transformation into other crystalline phases when no additives were used (Sarkar and Mahapatra 2010). Polyethylene (PE) tubes were utilized to connect water paths in the entire system, with a flow rate of 50 cc/min adjusted by a needle valve. This small flow rate and diameter resulted in a low Reynolds number flow.

The scaling samples of calcium carbonate collected from the experiment were subjected to SEM (6330, JEOL, USA) and XRD (D8, Bruker, USA) analyses to investigate the particle size and morphology of calcium carbonate under different magnetic conditions. Additionally, commercial meters for calcium ion concentration (LQAUAtwin-Ca-11, Horiba, Japan), pH value (F-71, Horiba, Japan), and electrical conductivity (DS-71, Horiba, Japan) were used to observe subtle changes during the experiment.

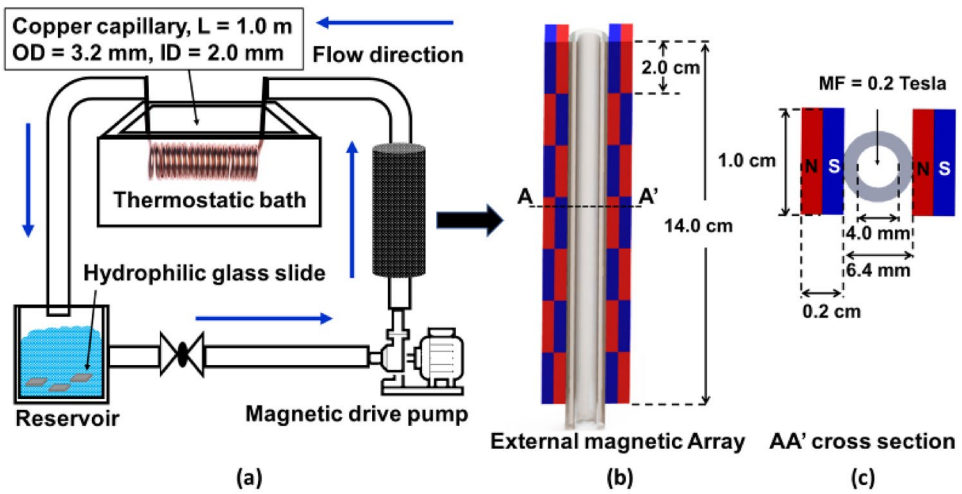

Fig. 1 The schematic diagram of **a** the experimental architecture, **b** the external magnetic array, and **c** the AA′ cross-sectional view of the external magnetic array

2.2 External magnetic array

The external magnetic array was composed of a series of pairs of neodymium magnets with north and south poles facing each other that are associated alternately (Gabrielli et al. 2001). The magnets were sized at $2.0 \times 1.0 \times 0.2$ cm^3, and arranged alternately as shown in Fig. 1b. Two different magnet lengths were used for the magnetic water treatment, which were 4.0 cm for 2 pairs of magnets and 14.0 cm for 7 pairs of magnets. The PE tube (with OD 6.4 mm and ID 4.0 mm) was combined with the magnets as depicted in Fig. 1c. It is also noted that the channel size of the external magnetic array, which corresponds to the magnetically treating area, is 4.0 mm, while the channel size of the copper capillary, which corresponds to the heating zone, is 2.0 mm. The solution was inside the PE tube and passed through the magnetic array, so the direction of the magnetic field was perpendicular to the direction of water flow (Kozic et al. 2003). The magnetic field strength of the external magnetic array was 0.2 Tesla, measured in the center of the PE tube using the Tesla meter (TM-801EXP, Kanetec, Japan). The magnetic field strength of the magnet used in this experiment was 0.3 T $\pm$ 10% on the north pole surface and the distance between the magnet pair was 6.4 mm, resulting in the magnetic gradient (0.05 T/mm $\pm$ 10%) across the tube for the anti-scale test.

3 Results and discussion

Table 1 depicts all the parameters applied to investigate the influence of the magnetic field on calcium carbonate formation. Regarding the water hardness classification for daily usage, the dissolved calcium carbonate concertation of greater than 150 mg/L is considered hard water (Alabi et al. 2015; Daesslé et al. 2009). In addition, the calcium carbonate hardness level should be lower than 500 mg/L for drinking water, regulated by World Health Organization (WHO) International Standards (Anbazhagan and Nair 2004). Therefore, the artificial hard water mixture of 3 mM sodium bicarbonate and 3 mM calcium chloride was chosen in this study to simulate the scale formation behavior in daily life. On the other hand, the higher concentration of 10 mM sodium bicarbonate and 10 mM calcium chloride solution was used for the accelerated scaling experiments. Except for the concentration, the temperature is another important factor to affect the solubility of calcium carbonate. When the temperature rises from 25 ℃ to 50 °C, the solubility drops by more than 30% (Coto et al. 2012). Therefore, the scale formation was observed in a short period in this study. Figure 2 presents the measured size distributions for the collected particles under different flow rates 50 cc/min, 100 cc/min and 150 cc/mm. The corresponding Reynolds numbers are 264, 528 and 792 for these flow rate in the magnet treating area. Results showed that the lower flow rates resulted in a longer treatment duration in laminar conditions. Therefore, this study set the flow rate of 50 cc/min for the rest experiments to have a longer treatment duration.

The concentration of calcium ions, the electric conductivity of total ions, and the pH value of test solutions were measured and recorded in the experiments, as shown in Figs. 3 and 4. During the 24-h treatment time, calcium ion concertation and electric conductivity dropped abruptly in the first 24 h, then slightly decreased until the equilibrium (Fig. 3). The solubility of calcium carbonate decreased when the temperature of the solution increased from room temperature 25 ℃ to 50 ℃. Once the calcium carbonate precipitated, the calcium ions were taken from the solution, causing a decrease in calcium ion concentration. It also was implied that calcium carbonate formation mostly occurred in the first 24 h. In addition, the conduction in ionic liquids was controlled by the movement of ions, so ions in test solutions decreased during calcium carbonate formation, resulting in a decrease in the electric conductivity. Furthermore, the scale is favorable to be formed in

Table 1 The experimental parameters for the test solutions

Concentration (mM)	Temperature (℃)	Flow rate (cc/min)	Magnetic field (T)	Magnet length (cm)	Treatment time (hr)
10	50	50	w/o	w/o	24
			0.2	4.0	24
			0.2	14.0	24
			0.2	14.0	72
3	50	50	w/o	w/o	24
			0.2	4.0	24
			0.2	14.0	24
			0.2	14.0	72

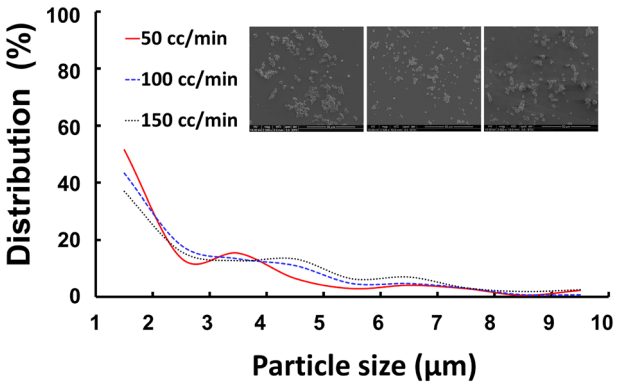

Fig. 2 Experimental results showing the collected particle distribution under different flow rates

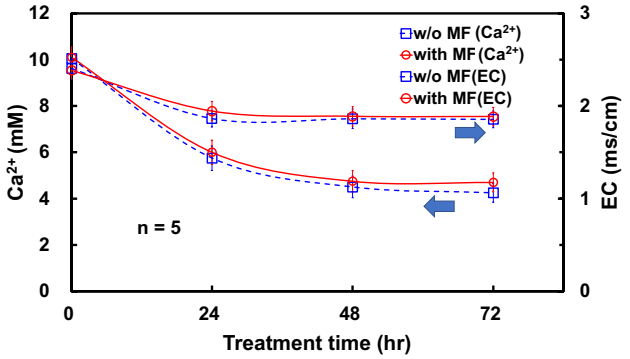

Fig. 3 The variation of calcium ion concentration and electrical conductivity during the 72-h treatment time for magnetic treated and untreated for 10 mM test solutions

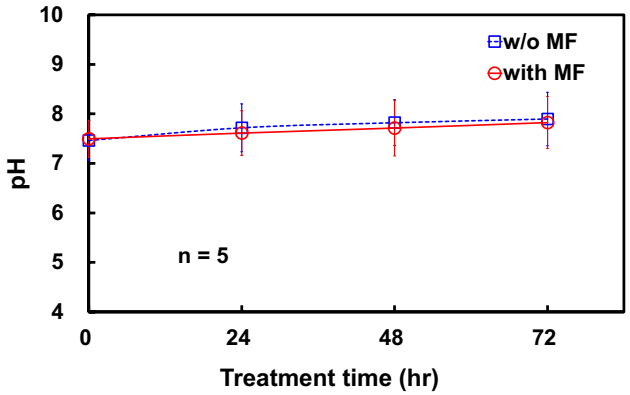

Fig. 4 The comparison of the pH measured value for magnetic treated and untreated for 10 mM test solutions during the 72-h treatment time

an alkaline solution, so pH is one important factor to be noticed during the precipitation of calcium carbonate. The measured pH of the treated and untreated solution both slightly increased after 72 h (Fig. 4). After calcium carbonate formation, bicarbonates in the test solution transformed to carbonate, so the pH value slightly increased. As the results of the measurements, there was no perceivable difference between the treated and untreated solutions, which meant the magnetic field did not alter the property of the test solutions.

The efficiency of the magnetic field influence on the scale formation is related to the solution exposure time to the magnetic field, which is affected by the length of magnets and treatment time. The exposure time t_{exp} of water to the magnetic field for n passes during treatment time t_T was described in Eq. (1), where s is the section area for the magnetic treatment, l is magnet length, and V is the total solution volume (Cai et al. 2009; Fathi et al. 2006). The equation infers that the longer magnet length and magnetic treatment time can increase the magnetic field exposure time to water.

$$t_{\text{exp}} = n\frac{sl}{V}t_T. \tag{1}$$

In this study, two different magnet lengths and magnetic treatment times were discussed to understand the efficiency of the magnetic field influence on calcium carbonate formation. The samples were collected at a controlled temperature (50 ℃) and flow rate (50 cc/min), when the solutions were experienced on the different magnet lengths (4.0 cm and 14.0 cm) and treatment time (24 h and 72 h). The SEM photographs (×2500) of calcium carbonate from 10 mM concentration and the PSD of calcium carbonate from both concentrations (10 mM and 3 mM) were obtained with the different magnetic conditions, as shown in Fig. 5. The various particle size with the different magnetic conditions were clearly observed in SEM photographs. To quantize the data, the PSD of calcium carbonate was obtained by the image processing program (ImageJ) with ×2500 SEM photos. Particles smaller than 1 µm were not considered in the analysis due to the pore size limitation of the membrane, which was 1 µm. The experimental results showed that the samples treated with a 3 mM solution and a magnet length of 14.0 cm for 24 h and 72 h exhibited particle sizes exclusively below 4 µm. Similarly, samples with a higher concentration of 1 mM, treated with a magnet length of 14.0 cm for 72 h, showed that all particles were smaller than 5 µm in size. On the contrary, the particle sizes were randomly distributed for the solutions without magnetic treatment. Therefore, the growth of calcium carbonate crystal size was inhibited by applying the external magnetic array. Moreover, for severer scaling situations such as 10 mM, increasing magnet length and treatment time led to a longer solution exposure time to the magnetic field, and then it increased the efficiency of the external magnetic array to process the solution with the high portion of smaller calcium carbonate particles. The possible mechanism for inhibiting crystal growth is based on thermodynamics. As ions move through the magnetic array, they encounter Lorentz forces due to their charged nature. These forces release energy into the test solution, causing an increase in the free energy of the thermal equilibrium system. As a result, the growth of calcium carbonate crystals is impeded, and the transformation of calcium carbonate into calcite with smaller particle sizes is promoted (Liang et al. 2022; Wang and Liang 2017).

The particle reduction rate due to the magnetic field influence is expressed as Eq. (2), where $D_{w/oMF}$ is the particle diameter of the sample without magnetic treatment, and D_{withMF} is the particle diameter of the sample with magnetic treatment.

$$\text{Reduction rate}(\%) = \frac{D_{w/o\text{MF}} - D_{\text{withMF}}}{D_{w/o\text{MF}}} \times 100\%. \tag{2}$$

Figure 6 shows the cumulative distribution of particle size for 3 mM test solutions with different magnetic conditions

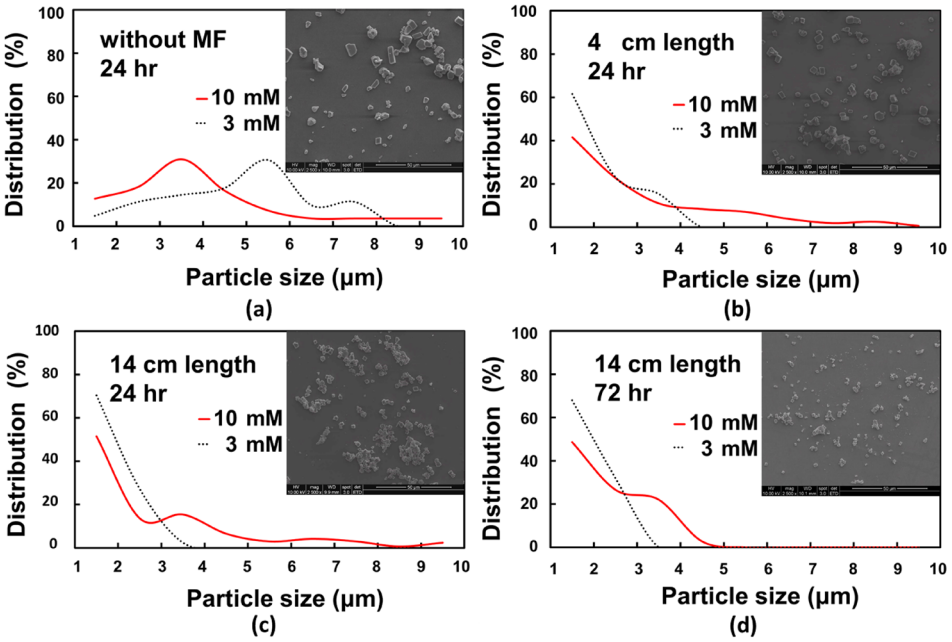

Fig. 5 The SEM photographs (×2500) of 10 mM test solutions and the PSD of $CaCO_3$ particles for both 10 mM and 3 mM test solutions, which conditions were **a** 24 h without magnetic treatment, **b** 24 h with magnetic treatment of 4.0 cm magnet length, **c** 24 h with magnetic treatment of 14.0 cm magnet length, and **d** 72 h with magnetic treatment of 14.0 cm magnet length

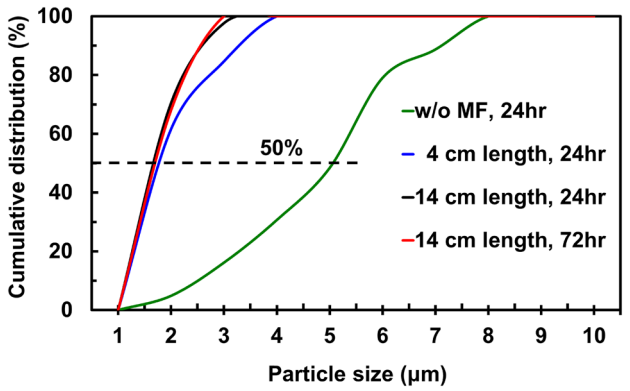

Fig. 6 The cumulative distribution of particle size for 3 mM test solutions with different magnetic conditions, which were 24 h without magnetic treatment, 24 h with magnetic treatment of 4.0 cm magnet length, 24 h with magnetic treatment of 14.0 cm magnet length, and 72 h with magnetic treatment of 14.0 cm magnet length, respectively

for comparison. The median particle diameter was obtained when the cumulative distribution reaches 50%, and it was considered a characteristic parameter as the average size of each condition to calculate the particle reduction rate in this study. The smallest median particle size was found in the solutions treated for 72 h with the magnet length of 14.0 cm, where the particle reduction rate was 66%. The cumulative particle distributions between the 24-h and 72-h treatment time with the magnet length of 14.0 cm were almost the same. It was indicated that the solution with 3 mM concentration completed the anti-scale process within 24 h by the external magnetic array with the magnet length of 14.0 cm. Compared to the particle reduction rate on the influence of the magnetic field in macro heat exchangers, their ultimate values were at 40% and 50% (Liang et al. 2022; Wang and Liang 2017). However, in the macrosystem, the diameter of the particle increased with increasing and decreasing magnetic induction intensities except in the ultimate condition. The particle size increased with an increase of the magnetic induction because that calcium carbonate formed a loose and irregular crystal structure (Zhao et al. 2014), which did not observe in our microfluidic channel heat exchange system.

The calcium carbonate phase identification was carried out by the X-ray diffraction technique. As shown in Fig. 7, the XRD patterns of calcium carbonate samples from 10 mM solutions were treated for 24 h with different magnet lengths, which were 4.0 cm, 14.0 cm magnet length, and without magnet, respectively. The peaks at 2θ equal to 23.0°, 29.4°, 31.7°, 36.0°, 39.4°, 43.2°, 47.5°, 48.50°, 56.6°, and 57.4° were attributed to the (102), (104), (006), (110), (113), (202), (108), (116), (211), and (212) planes of pure calcite (Al-Roomi et al. 2015; Wan et al. 2019; Zhou et al. 2004). All of them showed the strongest diffraction peaks at $2\theta = 29.4°$. The ratio of (110) plane slightly decreased when increasing the magnet length. On the other hand, the ratio of (116) plane increased when the magnet length increased. The results showed that the magnetic water treatment in the microfluidic channel slightly changed the crystal plane of calcite, and there was no aragonite found in the scale samples.

The SEM photographs (×10,000) of calcium carbonate were obtained from the 10 mM test solutions (Fig. 8). The calcium carbonate crystals without magnetic treatment were in the shape of a rhombus (Fig. 8a), and the particle size substantially decreased when the system was applied to the

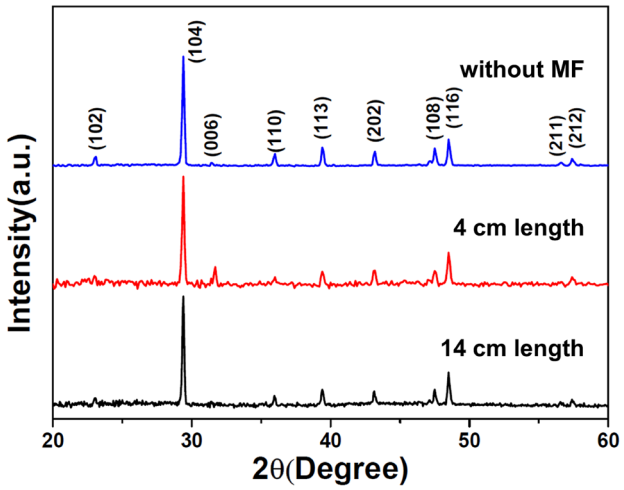

Fig. 7 The XRD patterns of 24 h treatment time for 10 mM test solutions with different magnet lengths: without magnetic treatment, with magnetic treatment of 4.0 cm magnet length, and with magnetic treatment of 14.0 cm magnet length

external magnetic array (Fig. 8b and c). As shown in Fig. 8c, the crystals with narrow rectangle shapes were found when the solutions were treated with the longer magnet length (14.0 cm). Compared to the test solutions, the particle sizes of the calcium carbonate without going through the heat exchange system were randomly distributed, and the crystal shapes were irregular (Fig. 8d). During the magnetic treatment, the orientation of ions was re-arranged (Al Helal et al. 2018), so the structure of calcium carbonate was slightly different during the formation, which corresponded to the XRD patterns of calcium carbonate samples with and without magnetic treatment.

4 Conclusion

The microfluidic channel that combined an external magnetic array was created to quickly examine the crystallographic morphology of calcium carbonate in this study. The influence of magnetic treatment on scale inhibition was evaluated by adjusting the magnet lengths and treatment times while controlling the flow rate and temperature. The results of this analysis were discussed. The PSD analysis revealed that utilizing a magnetic array with 14.0 cm length and applying it with treatment time of 72 h in both concentrations resulted in the production of the smallest particle sizes of calcium carbonate. By increasing the magnet length and treatment time, no inversion point in the reduction of particle size was observed, and particle reduction rates reached up to 66% for 3 mM test solutions, with all particles being smaller than 4 μm in size. Therefore, applying an

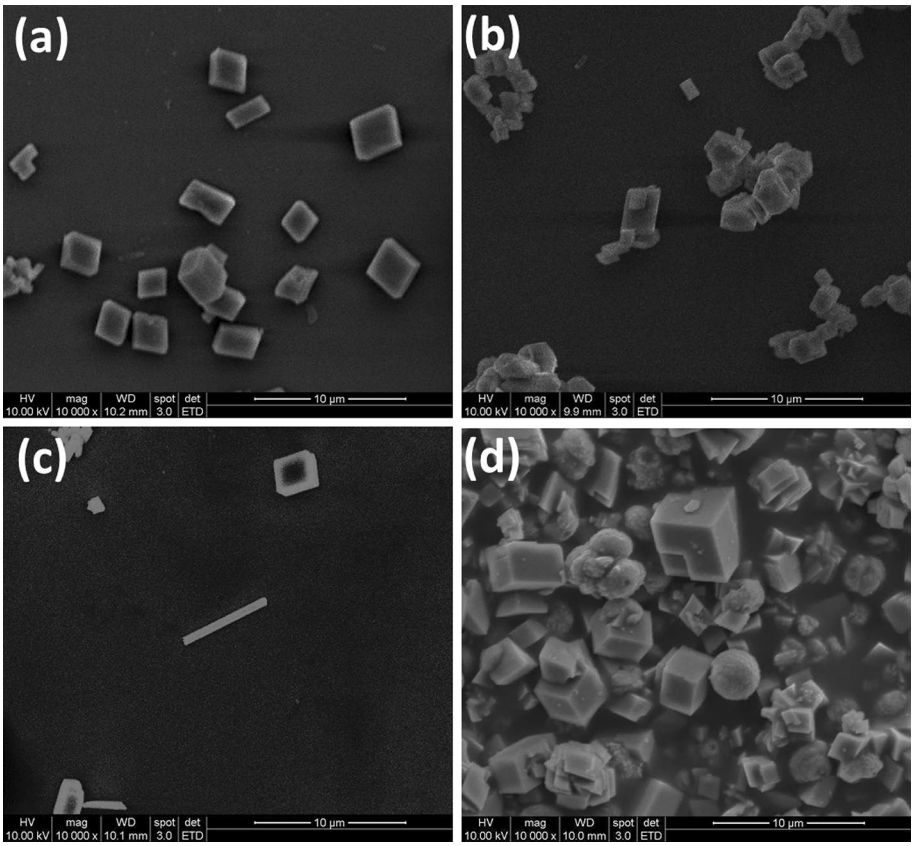

Fig. 8 The SEM photographs (×10,000) of 10 mM test solutions **a** treated for 24 h without applying magnet, treated for 24 h with applying magnetic treatment of **b** 4.0 cm and **c** 14.0 cm magnet length, and **d** $CaCO_3$ samples collected before going through the heat exchange system

external magnetic array to reduce the particle size can significantly decrease the scale problem in a microsystem. The XRD analysis revealed a slight alteration in the crystal plane of calcite due to the presence of a magnetic field within the microfluidic channel. All samples showed the strongest diffraction peaks of calcite at $2\theta = 29.4°$ (104) and the absence of aragonite. The SEM images displayed a narrow rectangular shape of the calcium carbonate crystal in the sample subjected to longer magnet length, indicating that ions might have been re-oriented upon passing through the magnetic field. Additionally, the measured values of calcium ion concentration, pH, and electrical conductivity provided insights into the subtle changes that occurred during calcium carbonate crystallization in each experiment. It was observed that the calcium ion concentration and electrical conductivity significantly decreased after 24 h of treatment time, while the pH increased slightly. However, there was no perceivable difference between the samples treated with and without the magnetic field, indicating that it did not alter the properties of the test solutions. The study successfully analyzed the crystallization behavior of calcium carbonate in a narrow channel under low Reynolds number flow, and the findings could be applied to minimize the scale problem in micro heat exchangers in the future.

Author contributions Chiung-Yi Huang wrote the main manuscript text and Che-Hsin Lin did the necessary revision.

Data availability Data supporting this study are openly available from Springer.

Declarations

Competing interests The authors declare no competing interests.

References

Al Helal A, Soames A, Gubner R, Iglauer S, Barifcani A (2018) Influence of magnetic fields on calcium carbonate scaling in aqueous solutions at 150 C and 1 bar. J Colloid Interface Sci 509:472–484

Alabi A, Chiesa M, Garlisi C, Palmisano G (2015) Advances in anti-scale magnetic water treatment. Environ Sci: Water Res Technol 1(4):408–425

Al-Roomi YM, Hussain KF, Al-Rifaie M (2015) Performance of inhibitors on $CaCO_3$ scale deposition in stainless steel & copper pipe surface. Desalination 375:138–148

Anbazhagan S, Nair AM (2004) Geographic information system and groundwater quality mapping in Panvel Basin, Maharashtra, India. Environ Geol 45:753–761

Baker JS, Judd SJ (1996) Magnetic amelioration of scale formation. Water Res 30(2):247–260

Benzinger W, Schygulla U, Jäger M, Schubert K (2005) Anti fouling investigations with ultrasound in a microstructured heat exchanger

Cai R, Yang H, He J, Zhu W (2009) The effects of magnetic fields on water molecular hydrogen bonds. J Mol Struct 938(1–3):15–19

Chibowski E, Szcześ A (2018) Magnetic water treatment—a review of the latest approaches. Chemosphere 203:54–67

Cho YI, Fan C, Choi B-G (1997) Theory of electronic anti-fouling technology to control precipitation fouling in heat exchangers. Int Commun Heat Mass Transfer 24(6):757–770

Cho YI, Fan C, Choi B-G (1998) Use of electronic anti-fouling technology with filtration to prevent fouling in a heat exchanger. Int J Heat Mass Transf 41(19):2961–2966

Cho YI, Lee S, Kim W, Suh S (2003) Physical water treatment for the mitigation of mineral fouling in cooling-tower water applications

Coey J, Cass S (2000) Magnetic water treatment. J Magn Magn Mater 209(1–3):71–74

Coto B, Martos C, Peña JL, Rodríguez R, Pastor G (2012) Effects in the solubility of $CaCO_3$: experimental study and model description. Fluid Phase Equilib 324:1–7

Daesslé L, Ruiz-Montoya L, Tobschall H, Chandrajith R, Camacho-Ibar V, Mendoza-Espinosa L, Lugo-Ibarra K (2009) Fluoride, nitrate and water hardness in groundwater supplied to the rural communities of Ensenada County, Baja California, Mexico. Environ Geol 58:419–429

Fathi A, Mohamed T, Claude G, Maurin G, Mohamed BA (2006) Effect of a magnetic water treatment on homogeneous and heterogeneous precipitation of calcium carbonate. Water Res 40(10):1941–1950

Gabrielli C, Jaouhari R, Maurin G, Keddam M (2001) Magnetic water treatment for scale prevention. Water Res 35(13):3249–3259

Hasson D, Shemer H, Sher A (2011) State of the art of friendly "green" scale control inhibitors: a review article. Ind Eng Chem Res 50(12):7601–7607

Hotrum NE, de Jong P, Akkerman JC, Fox MB (2015) Pilot scale ultrasound enabled plate heat exchanger—its design and potential to prevent biofouling. J Food Eng 153:81–88

Ignatov I, Mosin O (2014) Basic concepts of magnetic water treatment. Eur J Mol Biotechnol 4:72–85

Jiang P-X, Fan M-H, Si G-S, Ren Z-P (2001) Thermal–hydraulic performance of small scale micro-channel and porous-media heat-exchangers. Int J Heat Mass Transf 44(5):1039–1051

Jiang L, Zhang J, Li D (2015) Effects of permanent magnetic field on calcium carbonate scaling of circulating water. Desalin Water Treat 53(5):1275–1285

Jun P, Xuelong W, Haodong H, Shen Y, Qingsong X, Bin L (2018) Simulation for the dissolution mechanism of Cambrian carbonate rocks in Tarim Basin NW China. Pet Explor Dev 45(3):431–441

Kobe S, Dražić G, Cefalas AC, Sarantopoulou E, Stražišar J (2002) Nucleation and crystallization of $CaCO_3$ in applied magnetic fields. Cryst Eng 5(3–4):243–253

Kozic V, Lipus L (2003) Magnetic water treatment for a less tenacious scale. J Chem Inf Comput Sci 43(6):1815–1819

Lee C-Y, Wen C-Y, Hou H-H, Yang R-J, Tsai C-H, Fu L-M (2009) Design and characterization of MEMS-based flow-rate and flow-direction microsensor. Microfluid Nanofluid 6:363–371

Liang Y, Xu Y, Jia M, Wang J (2022) Experimental study on the influence of an alternating magnetic field on the $CaCO_3$ fouling of a heat transfer surface. Int J Heat Mass Transf 183:122156

MacAdam J, Parsons SA (2004) Calcium carbonate scale formation and control. Rev Environ Sci Biotechnol 3(2):159

Marshall JS, Renjitham S (2015) Simulation of particulate fouling at a microchannel entrance region. Microfluid Nanofluid 18:253–265

Martínez Moya S, Boluda Botella N (2021) Review of techniques to reduce and prevent carbonate scale. Prospecting in water treatment by magnetism and electromagnetism. Water 13(17):2365

Mayer M, Bucko J, Benzinger W, Dittmeyer R, Augustin W, Scholl S (2012) The impact of crystallization fouling on a microscale heat exchanger. Exp Thermal Fluid Sci 40:126–131

Mehendale S, Jacobi A, Shah R (2000) Fluid flow and heat transfer at micro-and meso-scales with application to heat exchanger design

Müller-Steinhagen H, Malayeri M, Watkinson A (2011) Heat exchanger fouling: mitigation and cleaning strategies. Heat Transfer Eng 32(3–4):189–196

Osman OO, Shintaku H, Kawano S (2012) Development of micro-vibrating flow pumps using MEMS technologies. Microfluid Nanofluid 13:703–713

Perry JL, Kandlikar SG (2008) Fouling and its mitigation in silicon microchannels used for IC chip cooling. Microfluid Nanofluid 5:357–371

Sarkar A, Mahapatra S (2010) Synthesis of all crystalline phases of anhydrous calcium carbonate. Cryst Growth Des 10(5):2129–2135

Silva IB, Neto JCQ, Petri DF (2015) The effect of magnetic field on ion hydration and sulfate scale formation. Colloids Surf, A 465:175–183

Tai CY, Wu C-K, Chang M-C (2008) Effects of magnetic field on the crystallization of $CaCO_3$ using permanent magnets. Chem Eng Sci 63(23):5606–5612

Wan C, Wang L-T, Sha J-Y, Ge H-H (2019) Effect of carbon nanoparticles on the crystallization of calcium carbonate in aqueous solution. Nanomaterials 9(2):179

Wang J, Liang Y (2017) Anti-fouling effect of axial alternating electromagnetic field on calcium carbonate fouling in U-shaped circulating cooling water heat exchange tube. Int J Heat Mass Transf 115:774–781

Xuefei M, Lan X, Jiapeng C, Zikang Y, Wei H (2013) Experimental study on calcium carbonate precipitation using electromagnetic field treatment. Water Sci Technol 67(12):2784–2790

Zhang Y, Shaw H, Farquhar R, Dawe R (2001) The kinetics of carbonate scaling—application for the prediction of downhole carbonate scaling. J Petrol Sci Eng 29(2):85–95

Zhao J-D, Liu Z-A, Zhao E-J (2014) Combined effect of constant high voltage electrostatic field and variable frequency pulsed electromagnetic field on the morphology of calcium carbonate scale in circulating cooling water systems. Water Sci Technol 70(6):1074–1082

Zhou G-T, Jimmy CY, Wang X-C, Zhang L-Z (2004) Sonochemical synthesis of aragonite-type calcium carbonate with different morphologies. New J Chem 28(8):1027–1031

Zhu JY, Suarez SA, Thurgood P, Nguyen N, Mohammed M, Abdelwahab H, Baratchi S (2019) Reconfigurable, self-sufficient convective heat exchanger for temperature control of microfluidic systems. Anal Chem 91(24):15784–15790